



BIROn - Birkbeck Institutional Research Online

Crawford, Ian (1991) Observations of interstellar lines towards HD 110432. *Astronomy & Astrophysics* 246 , pp. 210-212. ISSN 0004-6361.

Downloaded from: <https://eprints.bbk.ac.uk/id/eprint/28635/>

Usage Guidelines:

Please refer to usage guidelines at <https://eprints.bbk.ac.uk/policies.html>
contact lib-eprints@bbk.ac.uk.

or alternatively

Research Note

Observations of interstellar lines towards HD 110432

I. A. Crawford

Department of Physics and Astronomy, University College London, Gower Street, London WC1E 6BT, UK

Received October 30, accepted December 6, 1990

Abstract. High-resolution observations (3 km s^{-1} FWHM) of interstellar CH, CH^+ , Ca II and Na I towards the star HD 110432 are presented. The interstellar spectrum of this star is of particular interest as the line of sight passes through the Coalsack. The CH line was found to consist of two closely spaced velocity components, which is consistent with the velocity structure of the Coalsack determined from CO observations (Nyman et al. 1989). There is no significant velocity difference between the strongest CH component and the CH^+ line, which may be inconsistent with shock theories of CH^+ production.

Key words: interstellar clouds: Coalsack – interstellar molecules: CH, CH^+

1. Introduction

In an earlier paper (Crawford 1989a, henceforth “Paper 1”) observations were presented of interstellar lines towards the southern fifth magnitude star HD 110432. As discussed in that paper, the interstellar spectrum of this star is of particular interest as the line of sight passes through the Coalsack. The present paper presents new observations of CH and CH^+ , which were obtained at higher dispersion than those reported in Paper 1, and also presents a spectrum of the Na I D_2 line which may be compared with the Ca II K line obtained previously.

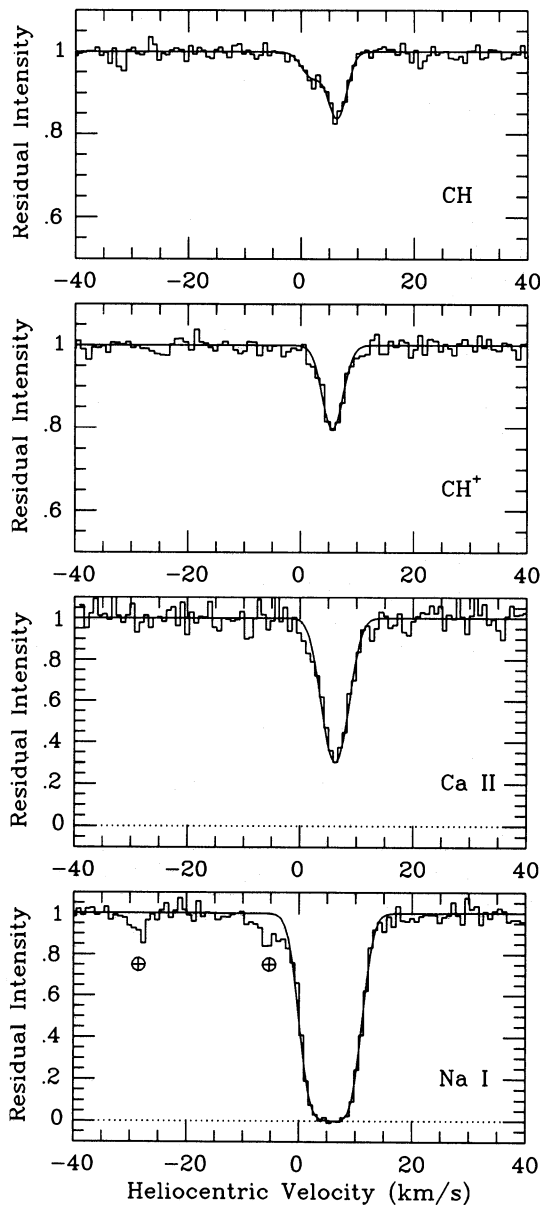
2. Observations and line profile analysis

The spectra were obtained using the coudé échelle spectrograph of the Mt Stromlo 74-inch telescope in 1990 June. The 130-inch focal length camera was used, resulting in a dispersion of 0.4 \AA mm^{-1} at the CH $\lambda 4300$ line; this is a factor of four better than employed for the CH and CH^+ observations reported in Paper 1. The adopted slit width was 250 \mu m , which gave a velocity resolution of 3 km s^{-1} (FWHM). The data reduction and calibration procedures employed were as described by Crawford (1990). The spectra were measured using the DIPSO program, described by Howarth & Murray (1988).

The spectra are shown in Fig. 1. The Ca II spectrum has been taken from Paper 1, and has been included here for comparison with the new observations. Superimposed on the observed spectra are theoretical line profiles calculated under the assumption of a Gaussian distribution of velocities; the theoretical profiles have been convolved with the instrumental response function to enable direct comparison with the observed data. The hyperfine splitting of the Na D_2 line, and the Λ -doubling of the CH $\text{R}_2(1)$ line, have been included in the model profiles. The adopted oscillator strengths are those tabulated by Crawford (1990). Table 1 gives the measured equivalent widths ($w_\lambda; 2\sigma$ errors), heliocentric radial velocity (v_{helio} ; determined from a least squares Gaussian fit, 1σ errors), the column density (N) and velocity dispersion (b) of the theoretical profiles shown in Fig. 1, together with the range in these values (ΔN , Δb) which give a satisfactory fit to the observed spectra. For lines which may be unresolved, an upper limit to b is given in Table 1; in such cases it is necessary to assume a lower limit for b in order to obtain an upper limit for N , and here a value of 0.3 km s^{-1} (corresponding to a temperature of 80 K in the absence of turbulence) has been adopted.

It is of interest to note that although the resolution employed here is only slightly higher than that used in Paper 1, the higher sampling rate (resulting from the larger dispersion) has clearly revealed the presence of a weaker component to the blue of the main CH line. This component is only marginally visible in the earlier spectrum, and a comparison between the present data and that presented in Paper 1 clearly shows the advantages that “over sampling” can have for the identification of weak and intrinsically narrow lines. This appears to be primarily due to the fact that, in an “over sampled” spectrum, even an unresolved line is significantly broader than the pixel to pixel variations, and can therefore be more easily distinguished from the noise.

The equivalent widths obtained here for the CH and CH^+ lines agree very well with those reported in Paper 1, although the errors on the present measurements are much lower. Moreover, the equivalent width obtained for the CH line, $13 \pm 2 \text{ m\AA}$ (summed over both velocity components), is in excellent agreement with the value of $12.3 \pm 0.5 \text{ m\AA}$ reported by van Dishoeck & Black (1989). There is little evidence for asymmetry in the line profile reported by van Dishoeck & Black (cf. their Fig. 7), but their observation of this line was obtained at somewhat lower resolution (4.3 km s^{-1} FWHM) than that adopted here.



3. Discussion

It is apparent from Table 1 that there is no significant velocity difference between the strongest CH component and the lines of CH⁺, Ca II and Na I. The data presented in Paper 1 were of insufficient quality to rule out a velocity difference between CH and CH⁺, but it is now clear that any difference must be very small (the values listed in Table 1 imply $v(\text{CH}) - v(\text{CH}^+) = 0.7 \pm 0.9 \text{ km s}^{-1}$ (1σ errors)). This is consistent with the results obtained from a study of CH and CH⁺ lines towards the Sco OB1 association (Crawford 1989b), and appears to be in conflict with shock theories of CH⁺ production (e.g. Elitzur & Watson 1980; Pineau des Forêts et al. 1986; Draine & Katz 1984) which predict a velocity difference of several km s^{-1} between the two species.

There is no convincing evidence for CH⁺, Ca II and Na I counterparts to the weaker ($v_{\text{helio}} = 1.9 \text{ km s}^{-1}$) CH component, and no attempt has been made to include such components in the model profiles shown in Fig. 1. Line profile modelling indicates that if such components are assumed to be present they have the following column density upper limits: $\lesssim 2 \cdot 10^{12} \text{ cm}^{-2}$ (CH⁺); $\lesssim 1 \cdot 10^{11} \text{ cm}^{-2}$ (Ca II); and $\lesssim 1 \cdot 10^{12} \text{ cm}^{-2}$ (Na I), where the large upper limit reflects the fact that a component at this velocity would be hidden in the blue wing of main, fully saturated, component. The detection of two components in CH, but only one in CH⁺, implies the existence of rather different CH⁺/CH ratios. Specifically, we have $0.9 \lesssim \text{CH}^+/\text{CH} \lesssim 1.8$ for the main ($v_{\text{helio}} = +6 \text{ km s}^{-1}$) component, and $\text{CH}^+/\text{CH} \lesssim 0.7$ for the weaker ($v_{\text{helio}} = +1.9 \text{ km s}^{-1}$) CH component. Similar variations of the CH⁺/CH column density ratio were found by Crawford (1989b) for the diffuse molecular clouds towards the Sco OB1 association.

The weighted mean heliocentric velocity of the main component is $+5.8 \pm 0.2 \text{ km s}^{-1}$. In the direction of HD 110432 vel-

←
Fig. 1. Observations of interstellar CH, CH⁺, Ca II K and Na I D₂ towards HD 110432. The observed spectra are plotted as histograms; the smooth curves are theoretical line profiles with the parameters given in Table 1. Weak atmospheric lines occur in the region of Na D, and the positions of these are indicated by ⊕ symbols

Table 1. Equivalent widths (w_λ), heliocentric velocities (v_{helio}), velocity dispersions (b) and column densities (N) for the observed lines. Δb and ΔN are the ranges of b and N which give acceptable fits to the observed line profiles. Where it was not possible to determine a lower limit to b from the line profile a value of 0.3 km s^{-1} was assumed in order to estimate the maximum value of N (see text). Powers of ten are given in parentheses

Line	λ_0 (Å)	w_λ (mÅ)	v_{helio} (km s^{-1})	b (km s^{-1})	Δb (km s^{-1})	N (cm^{-2})	ΔN (cm^{-2})
CH	4300.313	13 ± 2	$+1.9 \pm 1.5$	1.5	$\lesssim 2.5$	5.0 (12)	3.0–6.0 (12)
CH ⁺	4232.548	14 ± 2	$+6.4 \pm 0.7$	1.0	$\lesssim 1.5$	1.3 (13)	1.2–1.6 (13)
Ca II K	3933.663	56 ± 4	$+5.7 \pm 0.6$	1.8	$\lesssim 2.0$	1.7 (13)	1.4–2.2 (13)
Ca II K	3933.663	56 ± 4	$+6.2 \pm 0.3$	2.5	2.0–3.0	0.9 (12)	0.7–1.1 (12)
Na I D ₂	5889.950	228 ± 14	$+5.6 \pm 0.2$	2.8	1.5–3.5	1.5 (13)	0.5–60 (13)

ities relative to the local standard of rest (LSR) are 7.6 km s^{-1} more negative than heliocentric values. Thus the two components identified here have LSR velocities of $-5.7 \pm 1.5 \text{ km s}^{-1}$ and $-1.8 \pm 0.2 \text{ km s}^{-1}$. Dame et al. (1987) give a mean LSR radial velocity for the Coalsack of -4 km s^{-1} , which is close to the mean of these two values. From their detailed study of CO emission from the Coalsack, Nyman et al. (1989) found most of the emission to occupy the velocity range $-6 \leq v_{\text{LSR}} \leq 0 \text{ km s}^{-1}$ (cf. their Fig. 4). Thus the velocities obtained here are consistent with an origin in the Coalsack.

A careful comparison with the CO maps presented by Nyman et al. shows that HD 110432 ($l=302^\circ 0$, $b=-0^\circ 2$) lies outside the region of CO emission (as delineated by the 1 K km s^{-1} contour) over the LSR velocity range -6 to 0 km s^{-1} . This is not surprising since, as pointed out by the referee, the CH column densities inferred from the optical data are rather low for CO emitting regions. However, it is noteworthy that the line-of-sight passes much closer to the 1 K km s^{-1} contour (within $\sim 0.15 \text{ deg}$, or $\sim 0.46 \text{ pc}$) in the intervals -6 to -4 km s^{-1} and -2 to 0 km s^{-1} than in the interval -4 to -2 km s^{-1} , where it misses the 1 K km s^{-1} contour by $\sim 0.38 \text{ deg}$ (or 1.2 pc). We note that the former two velocity intervals include the velocities of the CH components identified here, while the latter lies between them. Thus, it appears that the CH components observed here arise in outlying diffuse gas associated with the denser CO emitting regions. The fact that the two components have different Ca II and Na I line strengths, and different CH^+/CH ratios, implies that these two clouds, while both being part of the Coalsack complex, nevertheless have different physical and/or chemical conditions. Weak CN absorption was detected towards this star by van Dishoeck & Black (1989); as the CN/CH ratio appears to be a diagnostic of cloud density (e.g. Federman et al. 1984), it would be of interest to obtain higher resolution observations of CN in order

to determine its abundance in each of the components identified in CH.

Finally, we note that the line-of-sight to HD 110432 passes very close to a dense clump (labeled "cloud 1" by Nyman et al. 1989) which has a LSR velocity of $+4.4 \text{ km s}^{-1}$ (or $+12 \text{ km s}^{-1}$ heliocentric). Owing to this anomalous positive velocity, Nyman et al. concluded that this clump is a background cloud, and not part of the Coalsack. The interstellar spectrum of HD 110432 shows no evidence for a component at this velocity, which supports this interpretation.

Acknowledgements. I thank the Mount Stromlo and Siding Spring Observatories for the allocation of time on the 74-inch telescope, and the UK Panel for the Allocation of Telescope Time (PATT) for the provision of travel money. I thank the referee for comments on an earlier draft of the manuscript.

References

- Crawford I.A., 1989a, Observatory 109, 232 (Paper 1)
 Crawford I.A., 1989b., MNRAS 241, 575
 Crawford I.A., 1990, MNRAS 243, 593
 Dame T.M., Ungerechts H., Cohen R.S., de Geus E.J., Grenier I.A., May J., Murphy D.C., Nyman L.-Å., Thaddeus P., 1987, ApJ 322, 706
 Draine B.T., Katz N.S., 1986, ApJ 310, 392
 Elitzur M., Watson W.D., 1980, ApJ 236, 172
 Federman S.R., Danks A.C., Lambert D.L., 1984, ApJ 287, 215
 Howarth I.D., Murray J., 1986, Starlink User Note, No. 50.11
 Nyman L.-Å., Bronfman L., Thaddeus P., 1989, A&A 216, 185
 Pineau des Forêts G., Flower D.R., Hartquist T.W., Dalgarno A., 1986, MNRAS 220, 801
 van Dishoeck E.F., Black J.H., 1989, ApJ 340, 273